Communication

Protein#Protein Interaction Detection in Vitro and in Cells by Proximity Biotinylation

Marta Ferna#ndez-Sua#rez, T. Scott Chen, and Alice Y. Ting

J. Am. Chem. Soc., **2008**, 130 (29), 9251-9253 • DOI: 10.1021/ja801445p • Publication Date (Web): 27 June 2008

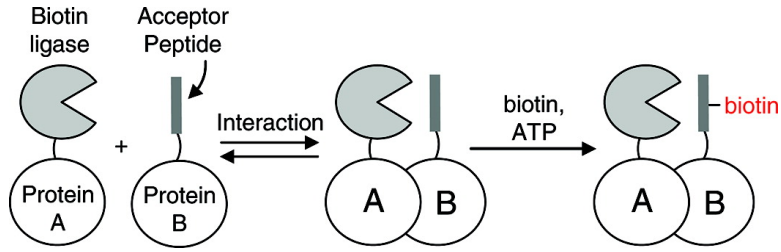

More About This Article

Additional resources and features associated with this article are available within the HTML version:

- Supporting Information
- Links to the 3 articles that cite this article, as of the time of this article download
- Access to high resolution figures
- Links to articles and content related to this article
- Copyright permission to reproduce figures and/or text from this article

View the Full Text HTML

J|A|C|S
COMMUNICATIONS

Published on Web 06/27/2008

Protein−Protein Interaction Detection in Vitro and in Cells by Proximity Biotinylation

Marta Fernández-Suárez, T. Scott Chen, and Alice Y. Ting*

Department of Chemistry, Massachusetts Institute of Technology, 77 Massachusetts Avenue, Cambridge, Massachusetts 02139

Received February 26, 2008; E-mail: ating@mit.edu

Networks of protein−protein interactions (PPIs) underlie all signaling pathways in cells. PPIs are commonly detected by purification and analysis of protein complexes from cell lysates, but methods that detect interactions within living, intact cells are preferable because they preserve spatial and temporal information and detect genuine PPIs in the context of native physiology. Live cell PPI detection methods include fluorescence resonance energy transfer (FRET)[1] and protein complementation assays (PCAs).[2] The major shortcoming of FRET for PPI detection is limited sensitivity and dynamic range.[3] In PCAs, which include split-GFP (green fluorescent protein),[4] split-β-lactamase,[5] and split-luciferase,[6] two halves of a reporter protein are separately fused to each interaction partner, and reporter activity or fluorescence is restored by PPI-induced reporter recombination. The major problem with PCAs is their high rate of false positives and false negatives. False positives can arise because most reporter halves have high intrinsic affinity for one another. False negatives emerge because reporter halves can sterically block PPIs and because many reporter fusion sites are not compatible with productive reporter recombination. Certain PCA systems have additional drawbacks, such as a time delay when using split-GFP due to fluorophore maturation or the loss of spatial resolution when using diffusible substrates of split-β-lactamase. Due to these limitations, new live cell PPI detection methods are needed, which offer high sensitivity and high spatiotemporal resolution, while also preserving high accuracy.

Here we report new methodology for PPI detection in cells, which overcomes some of the limitations of existing methods. Instead of using two halves of a reporter protein as in PCAs, we make use of an enzyme/substrate pair. One protein of interest is fused to the *Escherichia coli* enzyme biotin ligase (BirA), while another protein is fused to BirA's "acceptor peptide"[7] (AP) substrate (Figure 1A). If the two proteins A and B interact, BirA will catalyze site-specific biotinylation of AP, and we can detect biotinylated AP either by streptavidin staining of fixed cells[8] or streptavidin blotting of cell lysate.[9,10] Although the detection occurs on lysed or fixed cells, the labeling of the PPI of interest occurs within live cells, and thus physiology is not perturbed and transient interactions can in principle be identified. Our reporter design relies on the specificity of the BirA/AP pair. Inside mammalian cells, bacterial BirA enzyme does not biotinylate any endogenous proteins,[10,11] and conversely, the AP is not recognized by the mammalian biotin ligase.[9] Thus AP biotinylation can only result from the close proximity of BirA.

We first tested our proximity biotinylation strategy for PPI detection using the well-studied FKBP (FK506 binding protein)/FRB (FKBP−rapamycin binding protein) protein pair, whose interaction is regulated by the small molecule rapamycin.[12] The crystal structure of the ternary FKBP/rapamycin/FRB complex shows that the protein C-terminal ends are only ~18 Å apart,[13] and thus we prepared the C-terminal fusion constructs FKBP−AP and FRB−BirA (Figure 1B). When we expressed, purified, and tested these fusion proteins in vitro, we observed 5-fold greater biotinylation of FKBP−AP in the presence versus absence of rapamycin, as measured by streptavidin blot (Figure S1A).

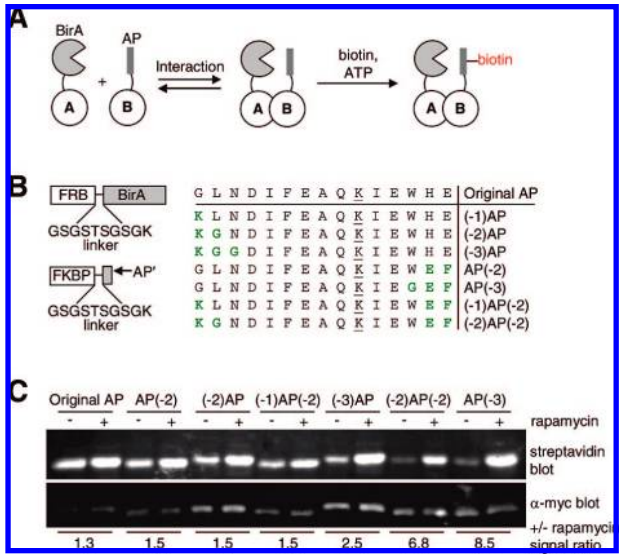

Figure 1. Protein−protein interaction detection with biotin ligase and an engineered acceptor peptide substrate. (A) Detection scheme. Interaction between proteins A and B results in site-specific biotinylation of the acceptor peptide (AP) by biotin ligase (BirA). (B) Left: domain structures of constructs used for in vitro and cellular tests. Right: FKBP was fused to the original AP sequence as well as to seven truncated variants of the AP with increased K_m for BirA. The lysine biotinylation site is underlined. Placeholder amino acids inserted at truncation sites are colored green. (C) Comparison of AP truncation mutants in a live cell assay. HEK cells co-transfected with FRB−BirA and one of the FKBP fusions to a truncated AP (FKBP−AP′) were either treated with 100 nM rapamycin for 1 h or left untreated. Biotin was then added for 1 min before lysis and analysis by streptavidin Western blot. The lower anti-myc blot visualizes the myc tag in each FKBP−AP′ construct.

Encouraged by these results, we repeated the experiment in live human embryonic kidney (HEK) cells. We incubated HEK cells expressing FRB−BirA and FKBP−AP(-3) with or without rapamycin for 1 h, then added biotin for 1 min, before cell lysis and analysis of biotinylated proteins by streptavidin blotting. Figure 1C (first two lanes) shows that the FKBP−AP biotinylation level was only 1.3-fold higher in cells treated with rapamycin compared to untreated cells. We surmised that inside cells, FKBP−AP and FRB−BirA expression levels are much higher than the protein concentrations we used in our in vitro experiments (1 μM). The K_m of AP for BirA is 25 μM,[7] and at FKBP−AP and FRB−BirA concentrations approaching this value, we would expect a high degree of PPI-independent biotinylation of AP. To remove this

background, we needed to reduce the intrinsic affinity of AP for BirA, ideally without decreasing the k_{cat} of biotinylation too much.

To reduce the affinity of AP for BirA, we prepared a series of truncated AP sequences. Up to three amino acids were removed from one or both ends of AP to decrease its interaction surface area with BirA. These sequences were fused to FKBP to give the FKBP−AP′ constructs shown in Figure 1B, and then we expressed them in live HEK cells with the original FRB−BirA construct. Analysis of the FKBP−AP′ biotinylation levels with and without rapamycin treatment showed that all the AP truncations decreased the background biotinylation level in the absence of rapamycin (Figure 1C). However, for many constructs, the biotinylation signal also decreased in the presence of rapamycin, leading to only small improvements in the ±rapamycin signal ratio. The AP(-3) construct, with three amino acids deleted from the C-terminal end of AP, was different; although the −rapamycin signal was reduced, the +rapamycin signal was comparable to that obtained with the original AP (signal/background ratio ∼8.5). We selected this new peptide for further characterization.

First, we repeated our cellular experiments, alongside negative controls to test the specificity of the detection. We found that biotinylation of FKBP−AP(-3) was eliminated when the lysine modification site in AP(-3) was mutated to alanine, when an inactive mutant of BirA was used (K183R), or when biotin was not added to the cells (Figure S2A). Second, we evaluated our method at different protein expression levels, both to check the sensitivity limits of our detection and to evaluate the signal/background ratios at different protein concentrations (Figure S3). We varied the FKBP−AP(-3) and FRB−BirA expression levels in HEK cells using a tetracycline-inducible expression system. Even at our lowest tetracycline concentration (0.1 μg/mL), giving the lowest protein expression, we could clearly detect rapamycin-dependent biotinylation of FKBP−AP(-3). The ±rapamycin signal ratio was highest (up to 28) when protein levels were lowest, consistent with the expectation that non-PPI-dependent biotinylation should be minimized at low BirA/AP expression levels. We also tested the BirA/AP(-3) pair using purified proteins in vitro and confirmed high detection sensitivity at low protein concentrations (Figure S1B).

We measured the kinetics of our new BirA/AP(-3) pair, using previously established assays[14] (Figure S2B). We found that the K_m increased significantly, from 25[7] to 345 ± 19 μM (14-fold). This explains our reduced background in cellular experiments. The k_{cat} also changed, an undesirable result, from 12[7] to 0.53 ± 0.01 min^{-1} (23-fold). However, due to the high sensitivity of our detection, we would still expect this impaired k_{cat} to permit labeling of PPIs with half-life greater than ∼1 min. To see if proximity biotinylation could be used to quantitate PPI strength, we performed a dose−response experiment, using varying rapamycin concentrations (Figure S2C). We found that the midpoint of the curve was 10 nM, which matches the previously reported in vitro K_d of the FKBP/rapamycin interaction with FRB.[15]

We were now ready to use proximity biotinylation to image PPIs in cells. Experiments were performed as above, but instead of cell lysis and streptavidin blotting, we fixed the cells and stained them with streptavidin conjugated to AlexaFluor 568. In addition, to minimize background biotin signal, both from endogenous substrates of mammalian biotin ligase[16] and from PPI-independent BirA recognition of AP, we depleted the culture media of biotin for 12 h prior to the experiment. Assays of mitochondrial respiration showed that such treatment was not toxic to cells (Figure S4).

Figure 2 shows that rapamycin-treated cells exhibited Alexa fluorescence, whereas untreated cells did not (signal/background ratio ∼5.1). We also stained the cells with anti-HA antibody to detect expression of FRB−BirA. The top row shows that only FRB−BirA-expressing cells displayed Alexa staining, while untransfected neighboring cells in the same field of view did not. We found that, in general, background biotinylation in the absence of rapamycin was essentially undetectable, despite high protein fusion expression levels due to the use of constitutive promoters. We also performed negative controls with mutated AP(-3) and mutated BirA and observed no biotinylation (Figure 2).

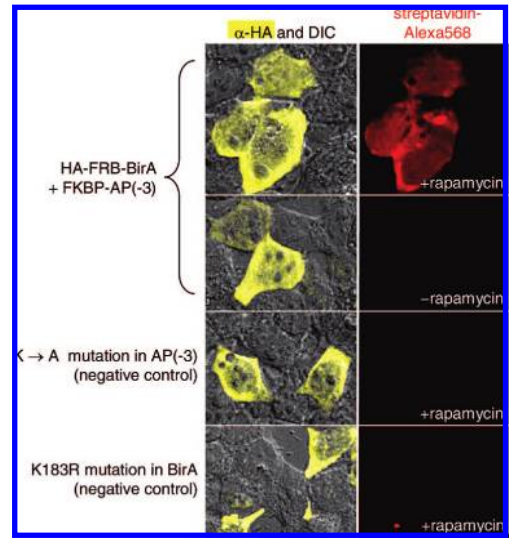

Figure 2. Imaging the FKBP/FRB interaction in cells. HEK cells were co-transfected with FRB−BirA and FKBP−AP(-3). After 3 h incubation with 100 nM rapamycin, cells were labeled with biotin for 1 min, then fixed and stained with streptavidin−AlexaFluor 568 (red). Anti-HA staining (yellow) shows HA−FRB−BirA expression. DIC (differential interference contrast) images on the left show total cells in the field of view. Negative controls are shown with rapamycin omitted, an alanine mutation in AP(-3), and a K183R mutation in BirA that eliminates its activity.

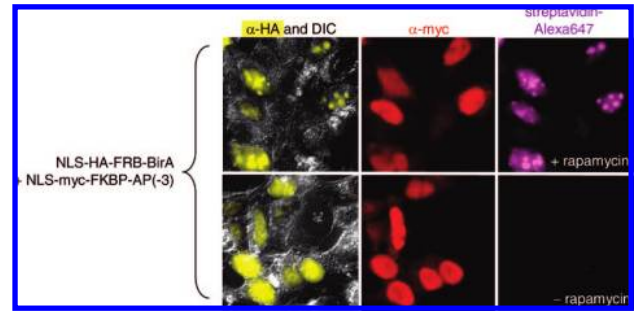

Figure 3. Proximity biotinylation provides subcellular localization of protein−protein interactions in cells. TRex−HEK cells were co-transfected with NLS−FRB−BirA and NLS−FKBP−AP(-3). NLS is a nuclear localization signal. Protein expression was induced with tetracycline for 24 h. Cells were labeled with biotin as above, then fixed and stained with streptavidin−AlexaFluor 647 (purple). Anti-HA staining (yellow) detects FRB expression, and anti-myc staining (red) detects total FKBP expression. Figure S5 shows results from imaging cells co-expressing untargeted FRB−BirA with NLS−FKBP−AP(-3), as well as cells co-expressing NLS−FRB−BirA with untargeted FKBP−AP(-3).

To illustrate how proximity biotinylation can reveal spatial patterns of PPIs in cells, we prepared nuclear-localized versions of FKBP−AP(-3) and FRB−BirA (these were fused to "nuclear localization signals", or NLS). When NLS−FKBP−AP(-3) was co-expressed with NLS−FRB−BirA, the Alexa signal highlighting biotinylation sites was localized to the nucleus (Figure 3). When only one construct (NLS−FRB−BirA) was nuclear-localized, while the other was both cytosolic and nuclear (FKBP−AP(-3)), we

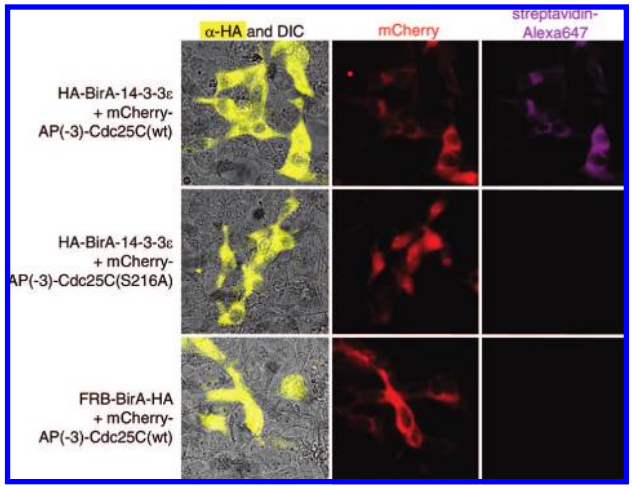

Figure 4. Imaging the interaction between Cdc25C and 14-3-3ε in cells. TRex−HEK cells were co-transfected with mCherry−AP(-3)−Cdc25C and BirA−14-3-3ε, and protein expression was induced with tetracycline for 24 h. Cells were then labeled with biotin for 1 min and fixed and stained with streptavidin−AlexaFluor 647 (purple). Anti-HA staining (yellow) detects total HA−BirA−14-3-3ε expression, and mCherry fluorescence (red) highlights Cdc25C. Controls are shown with the noninteracting S216A Ccd25C mutant and with BirA−14-3-3ε replaced by FRB−BirA.

observed only a nuclear Alexa signal (Figure S5A). The converse experiment, using FRB−BirA and NLS−FKBP−AP(-3), also produced only a nuclear signal (Figure S5B). These observations show, first, that biotin diffusion from the media to the nucleus is very fast. Second, BirA retains activity in the nucleus. Third, biotinylated AP(-3) redistributes minimally inside cells during the 1 min window between biotin addition to media and cell fixation, which allows preservation of spatial information about the PPI under study.

We also tested the generality of PPI imaging by using a different PPI pair. Cdc25C phosphatase interacts in a phosphorylation-dependent manner with the 14-3-3ε phosphoserine/threonine binding protein during the cell cycle.[17] We prepared an mCherry−AP(-3)−Cdc25C fusion construct and a BirA−14-3-3ε fusion construct, and we expressed these together inside HEK cells. Biotinylation was performed for 1 min in live cells, and the cells were fixed and stained with streptavidin−AlexaFluor 647 to detect biotinylated AP(-3)−Cdc25C. Figure 4 shows Alexa staining of transfected cells, indicated by their mCherry fluorescence (to visualize AP(-3)−Cdc25C expression) and HA staining (to visualize BirA−14-3-3ε expression). We also prepared a Cdc25C mutant, where the S216 phosphorylation site that mediates binding to 14-3-3ε was mutated to alanine. When this construct was coexpressed in HEK cells with 14-3-3ε, we observed no streptavidin staining. As expected, this mutation also changed Cdc25C localization from cytosolic to primarily nuclear.[17] An additional negative control with 14-3-3ε replaced by FRB showed that the biotin signal seen in the top row was dependent on 14-3-3ε.

In summary, we have developed a new method for PPI detection in vitro and in cells based on proximity biotinylation. The major advantages of our technique are the high sensitivity and low false positive rates across a wide range of protein expression levels. Compared to PCAs, our 12 amino acid AP(−3) tag is very small and thus less likely to inhibit PPIs. Our method can provide good spatial resolution, although biotinylated proteins could potentially redistribute during the 1 min biotin addition window. Even though we cannot image PPI dynamics, the rapid entry of biotin into cells combined with the fast rate of biotin ligation should enable the detection of relatively transient PPIs. We have demonstrated that proximity biotinylation can be applied to different protein pairs, although, as with PCAs, every new fusion construct must be tested and optimized for productive geometry. Finally, an important extension of any cellular PPI detection method is to the discovery of new protein interaction partners through library screens. Our method should be particularly well-suited for this application because the biotin label used for detection here can also serve as a handle for protein.

Acknowledgment. We thank Y. Zheng for assistance, M. Howarth for advice, and Tanabe U.S.A. for biotin. This work was supported by the NIH (R01 GM072670-01), and by the McKnight, Dreyfus, and Sloan Foundations.

Supporting Information Available: Supporting Figures 1−5, and all experimental details. This material is available free of charge via the Internet at http://pubs.acs.org.

References

(1) Truong, K.; Ikura, M. *Curr. Opin. Struct. Biol.* **2001**, *11*, 573–578.
(2) Remy, I.; Michnick, S. W. *Methods Mol. Biol.* **2004**, *261*, 411–426.
(3) Michnick, S. W. *Curr. Opin. Biotechnol.* **2003**, *14*, 610–617.
(4) Hu, C. D.; Kerppola, T. K. *Nat. Biotechnol.* **2003**, *21*, 539–545.
(5) Galarneau, A.; Primeau, M.; Trudeau, L. E.; Michnick, S. W. *Nat. Biotechnol.* **2002**, *20*, 619–622.
(6) Luker, K. E.; Smith, M. C.; Luker, G. D.; Gammon, S. T.; Piwnica-Worms, H.; Piwnica-Worms, D. *Proc. Natl. Acad. Sci. U.S.A.* **2004**, *101*, 12288–12293.
(7) Beckett, D.; Kovaleva, E.; Schatz, P. J. *Protein Sci.* **1999**, *8*, 921–929.
(8) Diamandis, E. P.; Christopoulos, T. K. *Clin. Chem.* **1991**, *37*, 625–636.
(9) de Boer, E.; Rodriguez, P.; Bonte, E.; Krijgsveld, J.; Katsantoni, E.; Heck, A.; Grosveld, F.; Strouboulis, J. *Proc. Natl. Acad. Sci. U.S.A.* **2003**, *100*, 7480–7485.
(10) Howarth, M.; Takao, K.; Hayashi, Y.; Ting, A. Y. *Proc. Natl. Acad. Sci. U.S.A.* **2005**, *102*, 7583–7588.
(11) Chen, I.; Howarth, M.; Lin, W.; Ting, A. Y. *Nat. Methods* **2005**, *2*, 99–104.
(12) Harris, T. E.; Lawrence, J. C., Jr *Sci. STKE* **2003**, re15.
(13) Choi, J.; Chen, J.; Schreiber, S. L.; Clardy, J. *Science* **1996**, *273*, 239–242.
(14) Chen, I.; Choi, Y. A.; Ting, A. Y. *J. Am. Chem. Soc.* **2007**, *129*, 6619–6625.
(15) Banaszynski, L. A.; Liu, C. W.; Wandless, T. J. *J. Am. Chem. Soc.* **2005**, *127*, 4715–4721.
(16) Chapman-Smith, A.; Cronan, J. E., Jr *Trends Biochem. Sci.* **1999**, *24*, 359–363.
(17) Dalal, S. N.; Schweitzer, C. M.; Gan, J.; DeCaprio, J. A. *Mol. Cell. Biol.* **1999**, *19*, 4465–4479.

JA801445P